Journal of Chemical Health Risks

www.jchr.org

JCHR (2025) 15(4), 2240-2246 | ISSN: 2251-6719

Role of MRI and MR Spectroscopy in the Evaluation of Ring Enhancing Lesions in Brain: A Cross-Sectional Observational Study

Dr.Vanshika Nandwani[1], Dr. Palak Marfatia[2], Dr. Rajesh Rathore[3], Dr. Harsh gaur[4]

[1]R3, Dept of Radiology, S.b.k.s medical College and research institute (sumandeep University)

[2]R3, Dept of Radiology, S.b.k.s medical College and research institute (sumandeep University)

[3]Head of the Department, Dept of Radiology, S.b.k.s medical College and research institute (sumandeep University)

[4]R3, Dept of Radiology, Kalinga institute of medical sciences (KIMS), Bhubaneswar

(Received: 29 June 2025 Revised: 31 July 2025 Accepted: 07 August 2025)

KEYWORDS

Brain neoplasms, Magnetic resonance imaging, Magnetic resonance spectroscopy, Neurocysticercosis, Ring-enhancing lesions, Tuberculoma

ABSTRACT:

Introduction: Ring-enhancing lesions of the brain are challenging neuroimaging abnormalities with diverse etiologies. Conventional MRI often faces limitations in differentiating between various pathologies, necessitating advanced techniques like MR spectroscopy for accurate diagnosis.

Aim: To study the characteristic imaging findings of various ring-enhancing lesions on MRI and evaluate the role of MR spectroscopy in their differentiation.

Materials and Methods: This cross-sectional observational study was conducted in the Department of Radiodiagnosis, Dhiraj General Hospital, Vadodara, Gujarat, from December 2022 to June 2023. Eighty patients diagnosed with ring-enhancing lesions on MRI were included. All patients underwent MRI brain with contrast and single-voxel proton MR spectroscopy using a 1.5 Tesla MRI machine. Metabolite ratios (Cho/Cr, Cho/NAA, NAA/Cr) and presence of specific peaks were analyzed.

Results: Mean age was 33.4±15.2 years with male predominance (56.3%). Seizures (65%) and headache (41.3%) were the most common presentations. Tuberculoma was the most frequent lesion (43.7%), followed by neurocysticercosis (28.7%), abscess (11.3%), metastasis (8.7%), and primary brain tumor (7.5%). On MR spectroscopy, tuberculomas showed lipid peaks in 82.8% ($p<0.001$), neurocysticercosis demonstrated choline peaks in 82.6% ($p<0.001$), while abscesses showed lactate peaks in 100% cases. The mean Cho/Cr ratio was significantly higher in primary brain tumors (5.1±1.32) and metastases (3.67±0.21) compared to infective lesions ($p<0.001$).

Conclusion: MRI with MR spectroscopy significantly improves the characterization and differentiation of ring-enhancing brain lesions. Specific metabolite patterns help distinguish between infective and neoplastic etiologies, facilitating appropriate management.

1. Introduction

Ring-enhancing lesions of the brain represent one of the most enigmatic neuroimaging abnormalities encountered in clinical practice. These lesions appear as areas of hypodensity or hypointensity surrounded by a rim of enhancement after contrast administration [1]. The differential diagnosis is extensive, including infectious causes like tuberculoma, neurocysticercosis, and pyogenic abscess; neoplastic lesions such as glioblastoma and metastases; and other conditions like demyelination and radiation necrosis [2].

The clinical presentation varies depending on the location, size, and etiology of the lesion. Common symptoms include seizures, headache, focal neurological deficits, and features of raised intracranial pressure. The causes of ring-enhancing lesions may differ between immunocompetent and immunocompromised individuals, further complicating the diagnostic process [3].

Journal of Chemical Health Risks
www.jchr.org
JCHR (2025) 15(4), 2240-2246 | ISSN: 2251-6719

Conventional MRI, despite being the gold standard for neuroimaging, often faces challenges in definitively characterizing these lesions. Similar imaging appearances between different pathologies, particularly tuberculoma and neurocysticercosis, can lead to diagnostic dilemmas. Advanced MRI techniques, including diffusion-weighted imaging and MR spectroscopy, have emerged as valuable tools to increase diagnostic specificity [4].

MR spectroscopy provides non-invasive information about tissue metabolism by detecting various metabolites such as N-acetyl aspartate (NAA), choline (Cho), creatine (Cr), lipids, and lactate. These metabolic signatures can help differentiate between various pathologies when conventional imaging remains inconclusive [5]. The present study aimed to evaluate the role of MRI and MR spectroscopy in characterizing various ring-enhancing lesions of the brain.

2. Materials and Methods

This cross-sectional observational study was conducted in the Department of Radiodiagnosis, Smt. B.K. Shah Medical Institute and Research Centre, Vadodara, Gujarat, from December 2022 to June 2023. The study was approved by the Institutional Ethics Committee (IEC/SBKSMIRC/2022/112).

Inclusion Criteria: The study will include patients of all age groups who have been diagnosed with ring-enhancing lesions on MRI and who are willing to participate in the research study and provide written informed consent.

Exclusion Criteria: Patients will be excluded from the study if they are post-operative cases or if they have contraindications to MRI or contrast administration.

Sample Size: Based on previous studies showing a prevalence of ring-enhancing lesions of approximately 15% among patients undergoing brain MRI, with 95% confidence interval and 5% margin of error, the calculated sample size was 78, rounded to 80 patients.

Data Collection: After obtaining written informed consent, detailed history including presenting complaints, duration of symptoms, and relevant past medical history was recorded. Socioeconomic status was assessed using the modified BG Prasad classification. All patients underwent complete neurological examination.

MRI Protocol: MRI brain with contrast was performed on a Philips 1.5 Tesla 16-channel MRI machine. The following sequences were obtained: T1-weighted (T1W), T2-weighted (T2W), Fluid Attenuated Inversion Recovery (FLAIR), Diffusion-Weighted Imaging (DWI) with Apparent Diffusion Coefficient (ADC) mapping, and post-gadolinium T1W sequences. Single-voxel MR spectroscopy was performed using Point Resolved Spectroscopy (PRESS) sequence with intermediate echo time (TE=135ms).

MR Spectroscopy Analysis: Voxel placement was done over the enhancing portion of the lesion, avoiding areas of necrosis or hemorrhage. Metabolite peaks for NAA (2.02 ppm), Cho (3.2 ppm), Cr (3.03 ppm), lipids (0.8-1.3 ppm), lactate (1.33 ppm), and amino acids were identified. Metabolite ratios (Cho/Cr, Cho/NAA, NAA/Cr) were calculated.

Follow-up: Final diagnosis was established through histopathological examination, response to specific treatment, or clinical follow-up with the treating physician.

Statistical Analysis

Data was entered in Microsoft Excel and analyzed using IBM SPSS version 25. Continuous variables were expressed as mean±standard deviation (SD), and categorical variables as frequencies and percentages. Chi-square test was used for comparing categorical variables between groups. ANOVA was used for comparing metabolite ratios between different lesion types. P-value <0.05 was considered statistically significant.

Journal of Chemical Health Risks
www.jchr.org
JCHR (2025) 15(4), 2240-2246 | ISSN: 2251-6719

3. Results

[Table/Fig-1]: CONSORT Flow Diagram

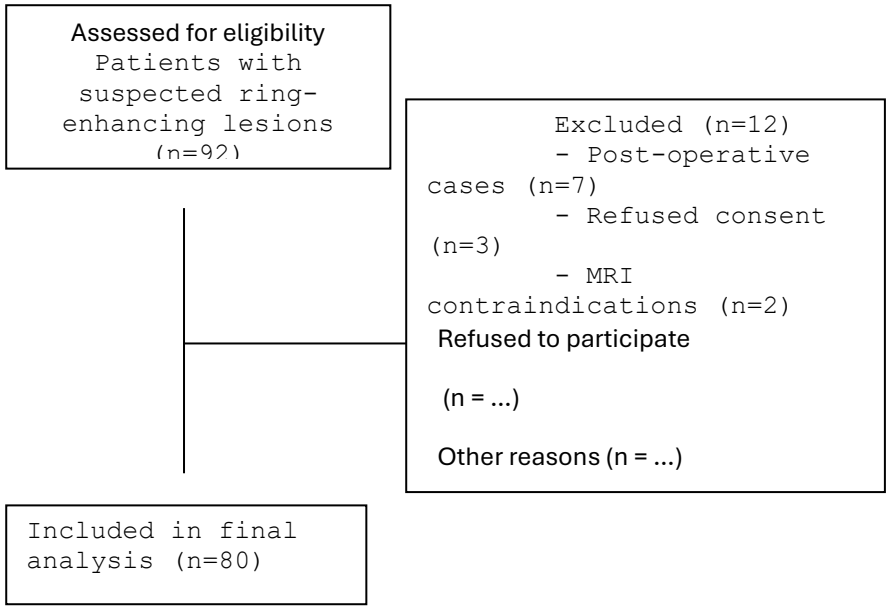

The study included 80 patients with ring-enhancing brain lesions. The flow of participants through the study is shown in [Table/Fig-1].

[Table/Fig-2]: Demographic characteristics of study population (n=80)

Parameter	Frequency (n)	Percentage (%)
Age groups (years)		
<15	9	11.3
16-30	29	36.2
31-45	19	23.7
46-60	15	18.8
>61	8	10.0
Gender		
Male	45	56.3
Female	35	43.7
Locality		
Rural	52	65.0
Urban	28	35.0

Journal of Chemical Health Risks
www.jchr.org
JCHR (2025) 15(4), 2240-2246 | ISSN: 2251-6719

Socioeconomic status		
Class I	12	15.0
Class II	15	18.7
Class III	21	26.3
Class IV	32	40.0

The demographic profile revealed that majority of patients (36.2%) were in the 16-30 years age group, with male predominance (56.3%). Most patients belonged to rural areas (65%) and lower socioeconomic status (Class IV: 40%).

[Table/Fig-3]: Clinical presentation and lesion characteristics

Parameter	Frequency (n)	Percentage (%)
Presenting symptoms		
Seizures	52	65.0
Headache	33	41.3
Fever	19	23.8
Vomiting	15	18.8
Neurological deficit	11	13.7
Ataxia	9	11.2
Type of lesion		
Tuberculoma	35	43.7
Neurocysticercosis	23	28.7
Abscess	9	11.3
Metastasis	7	8.7
Primary brain tumor	6	7.5
Number of lesions		
Single	30	37.5
2-4	29	36.3
>4	21	26.2
Size of lesions		
<2 cm	45	56.2
2-4 cm	22	27.5
>4 cm	13	16.3

Seizures were the most common presenting symptom (65%), followed by headache (41.3%). Tuberculoma was the most frequent diagnosis (43.7%), with majority of lesions being less than 2 cm in size (56.2%).

Journal of Chemical Health Risks
www.jchr.org
JCHR (2025) 15(4), 2240-2246 | ISSN: 2251-6719

[Table/Fig-4]: MRI morphological characteristics of ring-enhancing lesions

Lesion type	T1 hypointense n(%)	T1 isointense n(%)	T2 hypointense n(%)	T2 hyperintense n(%)	DWI restriction n(%)
Tuberculoma (n=35)	31(88.6)	4(11.4)	21(60.0)	6(17.2)	10(28.6)
Neurocysticercosis (n=23)	19(82.6)	4(17.4)	0(0)	20(86.9)	0(0)
Abscess (n=9)	9(100)	0(0)	0(0)	7(77.8)	9(100)
Metastasis (n=7)	5(71.4)	2(28.6)	0(0)	6(85.7)	5(71.4)
Primary brain tumor (n=6)	3(50.0)	1(16.7)	0(0)	4(66.7)	2(33.3)

Tuberculomas typically appeared hypointense on both T1 and T2-weighted images (88.6% and 60% respectively), while neurocysticercosis showed T1 hypointensity with T2 hyperintensity. All abscesses demonstrated diffusion restriction (100%), which was absent in neurocysticercosis cases.

[Table/Fig-5]: MR spectroscopy metabolite ratios in different lesions

Lesion type	Cho/Cr (Mean±SD)	Cho/NAA (Mean±SD)	NAA/Cr (Mean±SD)
Tuberculoma	1.60±0.41	1.40±0.49	1.32±0.39
Neurocysticercosis	1.20±0.20	1.34±0.36	1.11±0.32
Abscess	1.65±0.43	1.32±0.33	1.23±0.32
Metastasis	3.67±0.21[S]	2.10±0.61[S]	1.60±0.44
Primary brain tumor	5.10±1.32[HS]	3.44±0.78[HS]	1.33±0.42
p-value	<0.001	<0.001	0.087[NS]

Primary brain tumors and metastases showed significantly elevated Cho/Cr and Cho/NAA ratios compared to infective lesions ($p<0.001$). The highest Cho/Cr ratio was observed in primary brain tumors (5.10±1.32), distinguishing them from other pathologies.

[Table/Fig-6]: Distribution of metabolite peaks in various ring-enhancing lesions

Lesion type	Choline n(%)	Reduced NAA n(%)	Lipid n(%)	Lactate n(%)	Amino acids n(%)
Tuberculoma (n=35)	18(51.4)	12(34.3)	29(82.8)[HS]	21(60.0)	0(0)
Neurocysticercosis (n=23)	19(82.6)[S]	13(56.5)	6(26.1)	11(47.8)	0(0)
Abscess (n=9)	0(0)	6(66.7)	6(66.7)	9(100)[HS]	5(55.5)[S]
Metastasis (n=7)	7(100)[HS]	7(100)[HS]	3(42.8)	6(85.7)	0(0)

Journal of Chemical Health Risks
www.jchr.org
JCHR (2025) 15(4), 2240-2246 | ISSN: 2251-6719

Primary brain tumor (n=6)	6(100)[HS]	6(100)[HS]	3(50.0)	6(100)[HS]	0(0)

Tuberculomas characteristically showed lipid peaks in 82.8% of cases, while all abscesses demonstrated lactate peaks (100%). Neoplastic lesions (metastases and primary brain tumors) consistently showed elevated choline with reduced NAA (100% for both).

4. Discussion

Ring-enhancing lesions of the brain continue to pose diagnostic challenges despite advances in neuroimaging. The present study evaluated 80 patients to determine the role of MRI and MR spectroscopy in characterizing these lesions. The findings demonstrate that combining conventional MRI with MR spectroscopy significantly improves diagnostic accuracy.

The demographic profile in the present study showed a predominance of young adults (16-30 years: 36.2%) with male preponderance (56.3%), consistent with findings by Rajasree et al., who reported similar age distribution with peak incidence in the 21-30 years age group [6]. The higher prevalence in rural populations (65%) and lower socioeconomic groups (Class IV: 40%) reflects the epidemiological pattern of tuberculosis and neurocysticercosis in developing countries.

Seizures emerged as the most common presenting symptom (65%), followed by headache (41.3%), aligning with studies by Archana et al. (seizures: 50%) and Mishra et al. (headache: 65.5%, seizures: 40.6%) [7,8]. This symptom profile reflects the cortical and subcortical location of most ring-enhancing lesions.

Tuberculoma was the most frequent diagnosis (43.7%) in the present study, followed by neurocysticercosis (28.7%). This distribution differs from Western literature where neoplastic lesions predominate but is consistent with studies from endemic regions. Joy et al. reported neurocysticercosis as the most common lesion (59.2%) in their study from Karnataka, highlighting regional variations [9].

The MRI morphological characteristics proved valuable in initial differentiation. Tuberculomas typically appeared hypointense on both T1 and T2-weighted sequences (88.6% and 60% respectively), reflecting their solid caseating nature. This finding corroborates Ibrahim et al.'s observation that tuberculomas predominantly show T2 hypointensity [10]. In contrast, neurocysticercosis demonstrated T2 hyperintensity in 86.9% of cases, consistent with their cystic nature.

Diffusion-weighted imaging provided crucial information, with all abscesses showing restricted diffusion (100%) due to their purulent content, while neurocysticercosis showed no restriction. This finding aligns with established literature demonstrating the utility of DWI in differentiating abscesses from other cystic lesions [11].

MR spectroscopy emerged as a powerful tool for lesion characterization. The study revealed distinct metabolic signatures for different pathologies. Tuberculomas showed characteristic lipid peaks in 82.8% of cases, reflecting their lipid-rich caseous content. This finding supports previous studies by Gupta et al., who demonstrated elevated lipid peaks as a hallmark of tuberculomas [12].

Neurocysticercosis demonstrated elevated choline in 82.6% of cases with relatively preserved NAA levels, distinguishing them from neoplastic lesions. The presence of succinate and acetate peaks, though not consistently observed, when present, strongly suggested parasitic infection, as reported by Pretell et al. [13].

The metabolite ratio analysis revealed significant differences between lesion types. Primary brain tumors showed the highest Cho/Cr ratio (5.10±1.32), followed by metastases (3.67±0.21), both significantly higher than infective lesions ($p<0.001$). This elevation reflects increased membrane turnover and cellular proliferation in neoplastic lesions. The Cho/NAA ratio followed a similar pattern, with values >2 strongly suggesting malignancy.

Pyogenic abscesses demonstrated a unique spectroscopic profile with prominent lactate peaks (100%) and amino acid peaks (55.5%), representing anaerobic metabolism and proteolysis. The absence of normal brain metabolites helped differentiate abscesses from necrotic tumors, consistent with findings by Lai et al. [14].

The study findings have important clinical implications. The combination of conventional MRI features with MR spectroscopy can guide management decisions, potentially avoiding invasive procedures in cases with characteristic imaging-spectroscopic profiles. For instance, tuberculomas with typical T2 hypointensity and prominent lipid peaks can be confidently treated with anti-tubercular therapy without biopsy confirmation.

Limitations: The study had certain limitations. The cross-sectional design precluded assessment of treatment

Journal of Chemical Health Risks
www.jchr.org
JCHR (2025) 15(4), 2240-2246 | ISSN: 2251-6719

response. The single-center nature may limit generalizability to other populations. Some less common causes of ring-enhancing lesions like toxoplasmosis and lymphoma were not represented due to small sample size. Multi-voxel spectroscopy, which could provide spatial metabolic information, was not performed.

Future studies should focus on prospective evaluation of treatment response using serial MR spectroscopy. Integration of advanced techniques like perfusion imaging and machine learning algorithms may further improve diagnostic accuracy. Multi-center studies with larger sample sizes are needed to validate these findings across different populations.

5. Conclusion

MRI with MR spectroscopy significantly enhances the characterization of ring-enhancing brain lesions. Tuberculomas characteristically show T2 hypointensity with prominent lipid peaks, while neurocysticercosis demonstrates T2 hyperintensity with elevated choline. Neoplastic lesions exhibit markedly elevated Cho/Cr ratios (>3.5) with reduced NAA. Pyogenic abscesses show restricted diffusion with lactate and amino acid peaks. These distinct imaging-spectroscopic signatures enable accurate differentiation of various pathologies, facilitating appropriate management and potentially avoiding invasive diagnostic procedures.

References

1. Shetty G, Avabratha KS, Rai BS. Ring-enhancing lesions in the brain: A diagnostic dilemma. Iran J Child Neurol. 2014;8(3):61-64.
2. Garg RK, Sinha MK. Multiple ring-enhancing lesions of the brain. J Postgrad Med. 2010;56(4):307-16.
3. De Keersmaecker S, Van Cauter S, Bekelaar K. Multiple ring-enhancing brain lesions: Fulminant diffuse cerebral toxoplasmosis or cerebral metastases? Top Magn Reson Imaging. 2024;33(2):e0311.
4. Pope WB, Brandal G. Conventional and advanced magnetic resonance imaging in patients with high-grade glioma. Q J Nucl Med Mol Imaging. 2018;62(3):239-53.
5. Verma A, Kumar I, Verma N, Aggarwal P, Ojha R. Magnetic resonance spectroscopy - Revisiting the biochemical and molecular milieu of brain tumors. BBA Clin. 2016;5:170-78.
6. Rajasree D, Kumar TL, Vijayalakshmi K. Role of magnetic resonance spectroscopy in the evaluation of ring enhancing lesions of the brain. J Clin Diagn Res. 2020;14(10):TC10-TC15.
7. Archana R, Kumar P, Kishore A. Role of MRI in evaluation of ring enhancing lesions of brain in correlation with MR spectroscopy. Int J Contemp Med Surg Radiol. 2018;3(4):D121-25.
8. Mishra R. Role of MRI in characterisation of intracranial ring enhancing lesions in correlation with MR spectroscopy. Int J Contemp Med Res. 2022;9(6):F1-F6.
9. Joy L, Sakalecha AK. Role of multiparametric magnetic resonance imaging of the brain in differentiating neurocysticercosis from tuberculoma. Cureus. 2023;15(5):e39003.
10. Ibrahim IG, Osman AA, Shikhow MG, Celik C, Mutlu E, Hassan QM, et al. Magnetic resonance imaging findings of intracranial tuberculoma patients in a tertiary hospital in Mogadishu, Somalia: A retrospective study. Ann Med Surg. 2022;78:103812.
11. Reddy JS, Mishra AM, Behari S, Husain M, Gupta V, Rastogi M, et al. The role of diffusion-weighted imaging in the differential diagnosis of intracranial cystic mass lesions: A report of 147 lesions. Surg Neurol. 2006;66(3):246-50.
12. Gupta RK, Vatsal DK, Husain N, Chawla S, Prasad KN, Roy R, et al. Differentiation of tuberculous from pyogenic brain abscesses with in vivo proton MR spectroscopy and magnetization transfer MR imaging. AJNR Am J Neuroradiol. 2001;22(8):1503-09.
13. Pretell EJ, Martinot C Jr, Garcia HH, Alvarado M, Bustos JA, Martinot C. Differential diagnosis between cerebral tuberculosis and neurocysticercosis by magnetic resonance spectroscopy. J Comput Assist Tomogr. 2005;29(1):112-14.
14. Lai PH, Li KT, Hsu SS, Hsiao CC, Yip CW, Ding S, et al. Pyogenic brain abscess: Findings from in vivo 1.5-T and 11.7-T in vitro proton MR spectroscopy. AJNR Am J Neuroradiol. 2005;26(2):279-88.